A convex programming approach for color stereo matching

Wided Miled, Béatrice Pesquet-Popescu, Jean-Christophe Pesquet

A Convex Programming Approach for Color Stereo Matching

Wided Miled[1], Béatrice Pesquet-Popescu[1], Jean-Christophe Pesquet[2]

[1] *TELECOM ParisTech, Signal and Image Processing Department*
46 rue Barrault, 75634 Paris Cédex 13, France.
{miled, pesquet}@telecom-paristech.fr

[2] *Université Paris-Est, Institut Gaspard Monge and UMR-CNRS 8049*
5, Boulevard Descartes, Champs sur Marne, 77454 Marne-la-Vallée, France
jean-christophe.pesquet@univ-paris-est.fr

***Abstract*—This paper addresses the problem of dense disparity estimation from a pair of color stereo images. Based on a convex set theoretic formulation, the stereo matching problem is cast as a convex programming problem in which a color-based objective function is minimized under specific convex constraints. These constraints arise from prior knowledge and rely on various properties of the disparity field to be estimated. The resulting multi-constrained optimization problem is solved via an efficient parallel block-iterative algorithm. Four different color spaces have been tested in order to evaluate their suitability for stereo matching. Experiments on standard stereo images show that the matching results have been efficiently improved when using color information instead of grey values.**

I. Introduction

Stereo matching is a crucially important problem in computer vision with a wide range of applications, including multi-view video coding, multi-viewpoint generation, safe navigation and 3D television. The goal of stereo matching is to compute the disparity map between a pair of stereo images taken from distinct viewpoints. The disparity is defined as the difference in location between corresponding pixels, i.e. pixels resulting from the projection of the same 3D point onto the two image planes.

A broad range of approaches have been developed for solving the stereo matching problem. They are basically classified into three categories : feature-based, area-based and energy-based approaches. A good survey for the different stereo matching strategies is addressed in [1]. Feature-based methods [2] provide sparse disparity maps by matching extracted salient features from both images, such as edges, corners or segments. They have a low computational complexity and are well suited for real time processing tasks. In addition, they allow the recovery of large displacements and establish accurate disparity estimates. However, methods computing only sparse matches cannot be considered in many applications of stereo, such as view synthesis and 3D reconstruction. On the other hand, area-based methods produce dense disparity maps by correlation over local windows. They perform well in highly textured regions but often produce noisy disparities in textureless areas and fail around depth discontinuities. Many attempts have been made to solve these problems by varying the size and shape of the matching window according to the local variation of disparity characteristics [3], [4], [5]. Energy-based methods provide dense disparity fields by optimizing a global energy function, which is typically the sum of a data term and a smoothness term [6], [7], [8], [9], [10]. They are called global approaches and are generally more accurate than area-based approaches, especially in the challenging image regions.

In recent years, global optimization approaches have attracted much attention in the stereo vision community due to their excellent experimental results [1]. Many global stereo algorithms have, therefore, been developed dealing with ambiguities in stereo such as occlusions, depth discontinuities, lack of texture and photometric variations. These methods exploit various constraints on disparity such as smoothness, visibility, view consistency, etc., while using efficient and powerful optimization algorithms. Although many promising results have been obtained, an even accuracy may be achieved by using the color information, which is typically available in the stereo images.

Color provides much more distinguishable information than intensity values. Therefore, using color images in stereo matching yields more accurate estimates of disparity than grey value images. A number of different approaches have been proposed in the literature for color stereo matching. El Ansari et al. [11] proposed a new region based method for matching color images based on the fact that regions contain much richer information than individual pixels. To guarantee a great similarity between corresponding regions, a color-based cost function that takes into account the local properties of region boundaries is used. Koschan et al. [12] used a combination of a hierarchical block matching technique with active color illumination to improve the quality of the matching results, especially in homogenous regions. In [13], Mühlmann et al. have developed a real time and efficient method that calculates a correlation based dense disparity map from color stereo images. Alvarez and Sánchez [14] proposed a generalization of their work presented in [15], where they applied a PDE-based method for disparity estimation to color images. They modify the cost function so that it includes all three color components. Other color stereo techniques have been proposed in [16], [17], [18] and all have shown that the results have always been improved when using the color information. Most of the methods mentioned above commonly use the RGB color space. However, prior color evaluation studies [19], [20], [21] have shown that the precision of color stereo matching is improved only when a suitable color system is chosen.

In this paper, we propose a global variational method for computing a dense and accurate disparity map from a pair of color images. This method constitutes an extension of the technique we proposed in [10] to color stereo images. The stereo matching problem is solved through the minimization of a global objective function which is the sum of intensity differences over the three color channels in a predefined color space. Convex constraints introduced in [10] modelling prior knowledge on the disparity field remain available, except the Nagel-Enkelmann constraint which involves the left stereo image. A generalization of this constraint in the case of color images is proposed, inspired from [14]. Within a set theoretic framework, the stereo matching problem, formulated as a constrained optimization problem, is then solved via a parallel block-iterative decomposition method. Matching results with different color spaces are finally compared in order to determine the best performing color system.

The rest of the paper is organized as follows. In Section II, we introduce the color stereo model and describe the set theoretic formulation of the disparity estimation problem. Section III is devoted to presenting the objective function we minimize and the constraints we incorporate to the problem. In Section IV, we review the parallel block-iterative algorithm that will be employed to solve this problem. Experimental results on real stereo data sets are illustrated in Section V, followed by a conclusion in Section VI.

II. Problem formulation

A. Color stereo model

The stereo matching problem is to estimate a 2D disparity field by searching for every pixel in the left image the corresponding pixel in the right image. When stereo images are rectified [22], the vertical component of the disparity vector vanishes, so that only a scalar value has to be estimated. Let I_l and I_r be the left and right color images of a stereo pair, respectively. A color image may be represented as $I = \left(I^{(1)}, I^{(2)}, I^{(3)}\right)$, where $I^{(k)}, k \in \{1,2,3\}$, represents the k^{th} color channel in the selected color system. Finding a corresponding pixel in the right image I_r for each pixel in the left image I_l amounts to search the disparity u that minimizes the following cost function, based on the sum of color differences:

$$\tilde{J}(u) = \sum_{k=1}^{3} \sum_{(x,y)\in\mathcal{D}} [I_l^{(k)}(x,y) - I_r^{(k)}(x-u(x,y),y)]^2 \ , \quad (1)$$

where $\mathcal{D} \subset \mathbb{N}^2$ is the image support. This expression is non-convex with respect to the displacement field u. Thus, in order to avoid a non-convex minimization, we consider a Taylor expansion of the non-linear terms $\left\{I_r^{(k)}(x-\bar{u},y), k \in \{1,2,3\}\right\}$ around an initial estimate $\bar{u}$ as follows:

$$I_r^{(k)}(x-u,y) \simeq I_r^{(k)}(x-\bar{u},y) - (u-\bar{u})\nabla I_{r,x}^{(k)}(x-\bar{u},y) \ , \quad (2)$$

where $\nabla I_{r,x}^{(k)}(x-\bar{u},y)$ is the horizontal gradient of the warped right image channel $I_r^{(k)}$. Note that for notation concision, we have not made anymore explicit that u and $\bar{u}$ are functions of (x,y) in the above expression.

With the approximation (2), the cost function $\tilde{J}$ under the minimization in (1) becomes quadratic in u. Thus, setting $s = (x,y)$ the spatial position in either image, the objective function to be minimized can be rewritten as:

$$J(u) = \sum_{k=1}^{3} \sum_{s\in\mathcal{D}} [L^{(k)}(s) \ u(s) - r^{(k)}(s)]^2 \quad (3)$$

where

$$L^{(k)}(s) = \nabla I_{r,x}^{(k)}(x-\bar{u}(s),y)$$
$$r^{(k)}(s) = I_r^{(k)}(x-\bar{u}(s),y) + \bar{u}(s) \ L^{(k)}(s) - I_l^{(k)}(s).$$

B. Set theoretic formulation

Minimizing the objective function (3) aims at recovering the best estimate of the disparity image u from the observed fields $\{L^{(k)}\}_k$ and $\{r^{(k)}\}_k$. This inverse problem is ill-posed due to the fact that the components of $\{L^{(k)}\}_k$ may, simultaneously, vanish. Thus, to convert this problem to a well-posed one, it is useful to incorporate additional constraints modelling prior knowledge and available information on the solution. In the field of computer vision, such constraints were most commonly formulated as additional penalty terms in the objective function. In this work, the problem is addressed from a set theoretic formulation, where each constraint is represented by a convex set in the solution space and the intersection of these sets, the feasibility set, constitutes the family of possible solutions. The aim then is to find an acceptable solution minimizing the given objective function. A formulation of this problem in a Hilbert image space $\mathcal{H}$ is therefore:

$$\text{Find } u \in S = \bigcap_{i=1}^{m} S_i \text{ such that } J(u) = \inf J(S) \ , \quad (4)$$

where the objective $J : \mathcal{H} \to (-\infty, +\infty]$ is a convex function and the constraint sets $(S_i)_{1\le i\le m}$ are closed convex sets of $\mathcal{H}$. Constraint sets can generally be modelled as level sets:

$$\forall i \in \{1,\dots,m\}, \qquad S_i = \{w \in \mathcal{H} \mid f_i(w) \le \delta_i\} \ , \quad (5)$$

where, for all $i \in \{1,\dots,m\}$, $f_i : \mathcal{H} \to \mathbb{R}$ is a continuous convex function and $(\delta_i)_{1\le i\le m}$ are real-valued parameters such that $S = \bigcap_{i=1}^{m} S_i \neq \emptyset$.

The advantage of the convex program (4) is that a wide range of constraints modelling prior information can be explicitly incorporated to the problem as closed convex sets of the form (5). A further advantage of this formulation is to benefit from the availability of powerful optimization algorithms. For the current work, we employ the constrained quadratic minimization method recently developed in [23] and particularly well adapted to our needs.

III. Color stereo matching

In this section, we introduce the objective function as well as the considered convex constraints to solve the stereo matching problem from color stereo images, within the framework described above.

A. Global objective function

The objective function to be minimized is the quadratic measure (3) derived from our linearized color stereo model (see Section II). To cope with large deviations from the data model, occlusion points which are pixels only visible from one view of the stereo images have been detected and discarded in the expression of the similarity criterion. For a review of various approaches for finding occlusions, we refer to [24]. In this work, occlusion points were detected by enforcing the uniqueness and ordering constraints [25]. Furthermore, according to the conditions of convergence of the algorithm we use (see Section IV), the objective function J must be strictly convex. However, since the components of $\{L^{(k)}\}_k$ may vanish in (3), J is not secured to be strictly convex. We therefore introduce an additional strictly convex term as follows:

$$J(u) = \sum_{k=1}^{3} \sum_{\mathrm{s} \in \mathcal{D} \setminus \mathcal{O}} [L^{(k)}(\mathrm{s})\, u(\mathrm{s}) - r^{(k)}(\mathrm{s})]^2 + \alpha \sum_{\mathrm{s} \in \mathcal{D}} [u(\mathrm{s}) - \bar{u}(\mathrm{s})]^2 \; , \tag{6}$$

where $\mathcal{O}$ denotes the occlusion field, $\bar{u}$ is an initial estimate and α is a positive constant that weights the second term relatively to the first. The initial estimate $\bar{u}$ is obtained, first, from a correlation based method and, then, iteratively refined by choosing the result from a previous estimate as the initial value of the next step. This helps improving the quality of the solution while reducing the sensitivity of the final result to the initial estimate.

B. Convex constraints

1) Disparity range constraint: The most common constraint on disparity is the knowledge of its range of possible values. Indeed, disparity values are nonnegative and often have known minimal and maximal amplitudes, denoted respectively by $u_{\min} \geq 0$ and $u_{\max}$. The associated set is

$$S_1 = \{u \in \mathcal{H} \mid u_{\min} \leq u \leq u_{\max}\} \; . \tag{7}$$

2) Total variation regularization constraint: The smoothness constraint, initially introduced by Tikhonov [26], has been one of the most popular regularity assumptions. However, the Tikhonov regularization, by considering a quadratic function, tends to oversmooth discontinuities. In disparity estimation, we are interested in a regularization process that avoids smoothing around object boundaries. This can be achieved with the help of a suitable regularization constraint. In this work, we use a Total Variation based regularization constraint. Initially introduced by Rudin, Osher and Fatemi [27], this regularity measure has emerged as an effective tool to recover smooth images in variational image recovery [28], which naturally motivates its extension to the field of variational stereo methods [7], [10]. For a differentiable analog image defined on a domain Ω, the total variation is given by:

$$\mathrm{tv}(u) = \int_{\Omega} |\nabla u(s)|_2 \; ds \; , \tag{8}$$

where ∇u is the gradient of u and $|\cdot|_2$ denotes the Euclidean norm in $\mathbb{R}^2$. Practically, $\mathrm{tv}(u)$ represents a measure of the lengths of the level lines in the image. In a previous work [10], we have shown that the total variation $\mathrm{tv}(u)$ of the original disparity image u does not exceed some known bound τ. This constraint, which is associated with the set

$$S_2 = \{u \in \mathcal{H} \mid \mathrm{tv}(u) \leq \tau\} \; , \tag{9}$$

appears to be particularly relevant in stereo matching, as it smoothes homogenous regions in the disparity image while preserving edges. In addition, the upper bound τ can be estimated with good accuracy from prior experiments and the considered minimization method is shown to be robust with respect to the choice of this bound [28], [10].

3) Nagel-Enkelmann constraint: To benefit from the ability of the employed optimization algorithm to incorporate multiple constraints, we use another regularization constraint based on the Nagel-Enkelmann operator [29]. The oriented-smoothness ability of this operator has been primarily used in optical flow algorithms [29], [30] and has also been used for stereo in the variational framework of [15]. A formulation of the associated regularization term as a convex constraint set has been proposed in our previous work [10]. The main idea of this regularization constraint is that discontinuities in the disparity image are preserved accordingly to the edges of the left image I_l. An extension of this constraint, in the case of color images, can be defined as follows:

$$S_3 = \{u \in \mathcal{H} \mid \int_{\Omega} \big(\nabla u(s)\big)^{\top} D(\nabla \widehat{I}_l)(s)\, \nabla u(s)\, ds \leq \delta\} \; , \tag{10}$$

where δ is a positive constant. The Nagel-Enkelmann operator $D(\nabla \widehat{I}_l)$ is given by [14]:

$$D(\nabla \widehat{I}_l) = \frac{1}{|\nabla \widehat{I}_l|_2^2 + 2\gamma^2} \left\{ \begin{pmatrix} \frac{\partial \widehat{I}_l}{\partial y} \\ -\frac{\partial \widehat{I}_l}{\partial x} \end{pmatrix} \begin{pmatrix} \frac{\partial \widehat{I}_l}{\partial y} \\ -\frac{\partial \widehat{I}_l}{\partial x} \end{pmatrix}^{\top} + \gamma^2 \, \mathrm{I} \right\} ,$$

where I denotes the identity matrix, γ is the anisotropic diffusion constant and

$$\nabla \widehat{I}_l(s) = \nabla I_l^{(k_s)}(s), \text{ where } k_s = \arg \max_{k \in \{1,2,3\}} |\nabla I_l^{(k)}(s)|_2 \; .$$

The constraint S_3 has an isotropic behavior within uniform areas ($|\nabla \widehat{I}_l| \ll \gamma$), but at color edges ($|\nabla \widehat{I}_l| \gg \gamma$) it introduces an anisotropic smoothing to preserve the discontinuities.

IV. Optimization algorithm

The objective of this section is to develop a numerical solution to the problem of color stereo matching which has been formulated as a convex optimization problem. A parallel block iterative algorithm will be employed to efficiently minimize the quadratic objective function (6) over the feasibility set $S = \cap_{i=1}^{3} S_i$.

A. Subgradient projections

Here, we briefly recall the basic facts on subgradient projections which are necessary for our problem. More details can be found in [23]. The solution space is a real Hilbert space $\mathcal{H}$, endowed with the standard scalar product $\langle . \mid . \rangle$ and the associated Euclidean norm $\| \cdot \|$. Let S_i be the nonempty closed and convex subset of $\mathcal{H}$ given by (5), where f_i is a continuous and convex function. For every $u \in \mathcal{H}$, f_i possesses at least one subgradient at u, i.e., a vector $g_i \in \mathcal{H}$ such that

$$\forall\, z \in \mathcal{H}, \qquad \langle z - u \mid g_i \rangle + f_i(u) \le f_i(z)\ . \tag{11}$$

The set of all subgradients of f_i at u is the subdifferential of f_i at u and is denoted by $\partial f_i(u)$. If f_i is differentiable at u, then $\partial f_i(u) = \{\nabla f_i(w)\}$. Fix $u \in \mathcal{H}$ and a subgradient $g_i \in \partial f_i(u)$, the subgradient projection $P_i u$ of u onto S_i is given by:

$$P_i u = \begin{cases} u - \dfrac{f_i(u) - \delta_i}{\|g_i\|^2} g_i, & \text{if } f_i(u) > \delta_i; \\ u, & \text{if } f_i(u) \le \delta_i. \end{cases} \tag{12}$$

The proposed algorithm activates the constraints by means of subgradient projections rather than exact projections. The former are much easier to compute than the latter, as they require only the availability of a subgradient (the gradient in the differentiable case). However, when the projection is simple to compute, one can use it as a subgradient projection. In our case, exact projections onto S_1 is straightforwardly obtained, whereas a subgradient projection onto S_3 can be easily calculated. For the constraint S_2, the expression of a subgradient projection is given in [28].

B. Proposed algorithm

We now proceed to the description of the proposed block iterative algorithm to estimate the disparity u.

Algorithm 1:

① Fix $\varepsilon \in (0, 1/m[$ and set $n = 0$. Set

$$\begin{cases} \Phi(s) = \sum_{k=1}^{3} \left(L^{(k)}(s)\right)^2, \\ \Psi(s) = \sum_{k=1}^{3} L^{(k)}(s)\ r^{(k)}(s), \end{cases}$$

and compute u_0 as

$$u_0(s) = \begin{cases} \frac{\Psi(s) + \alpha\ \bar{u}(s)}{\Phi(s) + \alpha}, & \text{if } s \in \mathcal{D} \setminus \mathcal{O}, \\ \bar{u}(s), & \text{otherwise.} \end{cases}$$

② Take a nonempty index set $I_n \subseteq \{1, \ldots, m\}$.

③ For every $i \in I_n$, set $a_{i,n} = P_{i,n} - u_n$ where $P_{i,n}$ is a subgradient projection of u_n onto S_i as in (12).

④ Choose weights $\{\xi_{i,n}\}_{i \in I_n}$ in $(\varepsilon, 1]$ such that $\sum_{i \in I_n} \xi_{i,n} = 1$. Set $z_n = \sum_{i \in I_n} \xi_{i,n} a_{i,n}$ and $\kappa_n = \sum_{i \in I_n} \xi_{i,n} \|a_{i,n}\|^2$.

⑤ If $\kappa_n = 0$, exit iteration. Otherwise, set

- $b_n = u_0 - u_n$,
- c_n such that

$$c_n(s) = \begin{cases} (\Phi(s) + \alpha)\ b_n(s), & \text{if } s \in \mathcal{D} \setminus \mathcal{O}, \\ \alpha\ b_n(s), & \text{otherwise.} \end{cases}$$

- d_n such that

$$d_n(s) = \begin{cases} (\Phi(s) + \alpha)^{-1} z_n(s), & \text{if } s \in \mathcal{D} \setminus \mathcal{O}, \\ \alpha^{-1} z_n(s), & \text{otherwise.} \end{cases}$$

- $\lambda_n = \kappa_n / \langle d_n, z_n \rangle$.

⑥ Set $\tilde{d}_n = \lambda_n d_n$, $\pi_n = -\langle c_n, \tilde{d}_n \rangle$, $\mu_n = \langle b_n, c_n \rangle$, $\nu_n = \lambda_n \langle \tilde{d}_n, z_n \rangle$ and $\rho_n = \mu_n \nu_n - \pi_n^2$.

⑦ Set

$$u_{n+1} = \begin{cases} u_n + \tilde{d}_n, & \text{if } \rho_n = 0,\ \pi_n \ge 0; \\ u_0 + (1 + \frac{\pi_n}{\nu_n}) \tilde{d}_n, & \text{if } \rho_n > 0,\ \pi_n \nu_n \ge \rho_n; \\ u_n + \frac{\nu_n}{\rho_n} (\pi_n b_n + \mu_n \tilde{d}_n), & \text{if } \rho_n > 0,\ \pi_n \nu_n < \rho_n. \end{cases}$$

⑧ Increment n and go to step ②.

Theorem 2: Suppose that there exists a positive integer M such that

$$\forall\, n \in \mathbb{N}, \qquad \bigcup_{k=n}^{n+M-1} I_k = \{1, \ldots, m\}, \tag{13}$$

then every sequence $(u_n)_n$ generated by Algorithm 1 converges to the unique solution of (4).

Remarks 3: Algorithm 1 allows to easily incorporate additional convex constraints if these are available. Its ability to use approximate (subgradient) projections onto the constraint sets makes it possible to handle a wide range of complex convex constraints. In addition, it has been shown in [23] that, due to its block iterative structure, this algorithm offers a lot of flexibility in terms of parallel implementation. In particular, several processors can be used in parallel to compute the subgradient projections on the different constraint sets $(S_i)_{1 \le i \le m}$, leading to improved results while reducing the computational time.

V. Experimental results

In this section, we present results of the proposed method using standard data sets taken from the Middlebury Database. Figure 1 shows the four stereo pairs considered in this work along with their ground truth images. To parameterize our method, the parameter α in equation (6) and the anisotropic diffusion constant γ were set to 10 and 1, respectively. Bounds on the constraint sets $(S_i)_{1 \le i \le 3}$ were computed directly from ground truth fields (see Table I) and three cycles of iterations were performed to refine the initial disparity fields as described in Section III-A. The algorithm has been tested with the four color models RGB, LUV, LAB, $I_1I_2I_3$ and the grey level image representation. As ground truth fields are available for the considered stereo pairs, we evaluate the different results quantitatively by computing two error measures: the mean absolute error (MAE) between computed and ground truth fields and the percentage of bad matching pixels (Err) with absolute error larger than one pixel. Following [1], we only consider non-occluded pixels when computing the disparity errors. The overall results provided by our method for the different color spaces are shown in Table II(a), where we also indicate the rank of the color spaces according to their

Fig. 1. Left images (Top) of the considered stereo pairs and corresponding ground truth images (Down). From left to right: Venus, Teddy, Dolls, Baby.

MAE and Err errors. As we can see, the precision of the matching has generally been improved when using the color information, except for the Venus stereo pair where color seems to slightly worsen the results. For the other stereo pairs, the mean absolute error was significantly reduced when using the LUV, RGB and $I_1I_2I_3$ color spaces. However, no significant changes in the results have been noticed when using the LAB color space instead of the grey value information. Table II also includes, for comparison purposes, the results from the global optimization algorithm (GC) of Kolmogorov and Zabih [9] based on graph-cuts. The same observation about the obvious utility of color information in solving the stereo matching problem could be made when comparing the results of the grey value based matching of this method and the color based matching. We can also notice from Table II that the proposed method, compared to the (CG) algorithm, leads always to the best results.

In Figures 2 and 3, we show the disparity maps computed by the proposed and the (GC) methods for the three stereo pairs : Teddy, Dolls and Baby. These image pairs are more challenging than the Venus stereo pair, since they have complex scene structures, wide disparity ranges and large occluded regions. When only using grey values, the disparity maps are represented in Figures 2-3(b). The results of using the RGB and LUV color spaces are shown in Figures 2-3(c) and 2-3(d), respectively. As expected, many matching errors are reduced by using the color information. Especially, we notice that the most precise results have been generally obtained by using the LUV space, which seems to be a suitable color space for stereo matching.

VI. Conclusion

Stereo matching is a crucially important problem in computer vision. In this paper, we presented a convex programming approach for matching color stereo images. A robust and efficient optimization algorithm was developed to provide a reliable dense disparity map. Within a convex set theoretic framework, this algorithm minimizes a quadratic color-based objective function subject to some appropriate convex constraints. It can incorporate a wide range of additional constraints and is highly parallelisable due to its block iterative structure. Four different color spaces have been used and compared for the evaluation of matching results from color stereo images. The results indicate that stereo matching can be significantly improved by using a suitable color space. We found that the LUV color space offers the best performances for the considered test image pairs.

TABLE I
PARAMETER SETTINGS.

Stereo pair	τ	δ	disparity range
Venus	9×10^3	7×10^4	$[0,20]$
Teddy	4×10^4	1.2×10^5	$[15,55]$
Dolls	5×10^4	1.5×10^5	$[20,75]$
Baby	4×10^4	5×10^5	$[1545]$

TABLE II
COMPARATIVE RESULTS USING COLOR SPACES AND GREY LEVEL REPRESENTATION.

Color space	Venus MAE	Venus Err	Teddy MAE	Teddy Err	Dolls MAE	Dolls Err	Baby MAE	Baby Err
RGB	0.25_2	5_3	0.49_3	12_2	0.35_3	7_1	0.51_3	7_2
LUV	0.29_4	8_4	0.43_1	11_1	0.27_1	8_2	0.44_1	4_1
$I_1I_2I_3$	0.26_3	4_2	0.47_2	12_2	0.32_2	10_3	0.49_2	7_2
LAB	0.33_5	11_5	0.56_4	17_5	0.45_4	15_5	0.73_4	14_4
Grey	0.22_1	2_1	0.57_5	13_4	0.48_5	11_4	0.91_5	20_5

(a) Results from our method.

Color space	Venus MAE	Venus Err	Teddy MAE	Teddy Err	Dolls MAE	Dolls Err	Baby MAE	Baby Err
RGB	0.33_3	12_2	0.69_3	20_4	0.82_3	19_2	0.58_1	23_2
LUV	0.45_4	17_4	0.61_1	11_1	0.75_2	19_2	0.65_3	21_1
$I_1I_2I_3$	0.53_5	22_5	0.63_2	14_2	0.66_1	18_1	0.60_2	24_3
LAB	0.32_2	12_2	0.82_5	25_5	0.89_4	24_5	0.94_4	26_4
Grey	0.29_1	8_1	0.79_4	15_3	0.92_5	20_4	1.06_5	26_4

(b) Results from the (GC) method.

References

[1] D. Scharstein and R. Szeliski. A taxonomy and evaluation of dense two-frame stereo correspondence algorithms. *Int. J. Comput. Vis.*, 47(1):7–42, 2002.

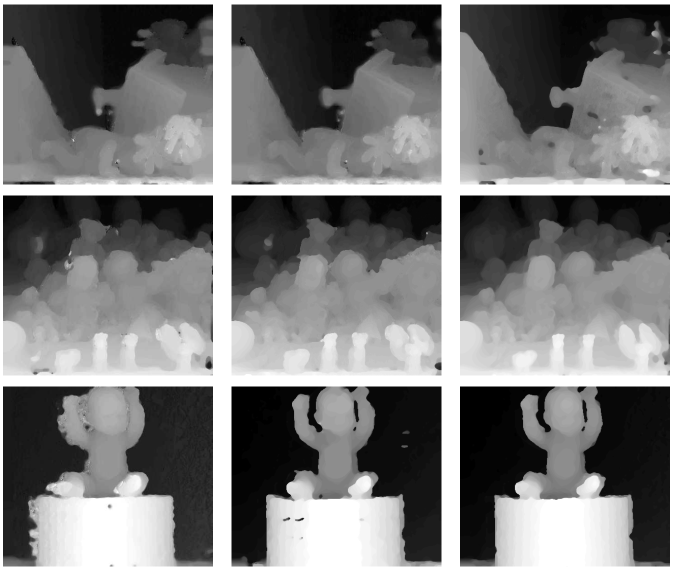

(a) Grey levels (b) RGB color space (c) LUV color space

Fig. 2. Disparity maps from our method applied on Teddy, Dolls and Baby stereo pairs.

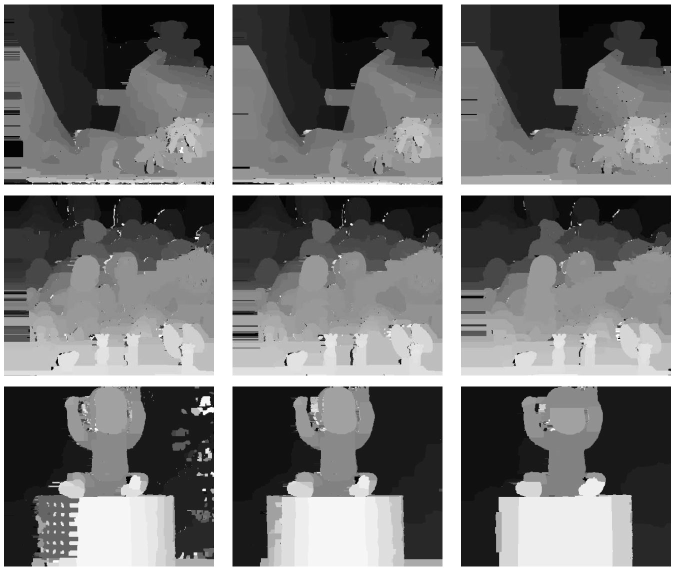

(a) Grey levels (b) RGB color space (c) LUV color space

Fig. 3. Disparity maps from the (GC) algorithm applied on Teddy, Dolls and Baby stereo pairs.

[2] O. Veksler. Semi-dense stereo correspondence with dense features. In *IEEE Workshop Stereo and Multi-Baseline Vision*, pages 149–157, Kauai, Hawaii, Dec. 2001.

[3] E. Izquierdo. Disparity/segmentation analysis: Matching with an adaptive window and depth-driven segmentation. *IEEE Trans. on Circuits and Systems for Video Technology*, 9(4):589–607, June 1999.

[4] A. Fusiello, V. Roberto, and E. Trucco. Symmetric stereo with multiple windowing. *Int. J. Pattern Recognit. Artifi. Intell.*, 14(8):1053–1066, 2000.

[5] M. Agrawal and L. Davis. Window-based, discontinuity preserving stereo. *Proc. Int. Conf. Comput. Vis. Pattern Recognit.*, 1:66–73, Jun. 2004.

[6] M. Bleyer and M. Gelautz. A layered stereo algorithm using image segmentation and global visibility constraints. *Int. Conf. Image Process.*, pages 2997–3000, 2004.

[7] N. Slesareva, A. Bruhn, and J. Weickert. Optic flow goes stereo: A variational method for estimating discontinuity-preserving dense disparity maps. *Pattern Recognition*, pages 33–40, 2005.

[8] O. Veksler. Stereo correspondence by dynamic programming on a tree. In *Proc. Int. Conf. Comput. Vis. Pattern Recognit.*, volume 2, pages 384–390, San Diego, US, Jun. 2005.

[9] V. Kolmogorov and R. Zabih. Computing visual correspondence with occlusions using graph cuts. In *Int. Conf. on Computer Vis.*, volume 2, pages 508–515, Vancouver, Canada, Jan. 2001.

[10] W. Miled, J.-C. Pesquet, and M. Parent. Disparity map estimation using a total variation bound. In *Proc. 3rd Canadian Conf. Comput. Robot Vis.*, pages 48–55, Quebec, Canada, Jun. 2006.

[11] M. El Ansari, L. Masmoudi, and A. Bensrhair. A new regions matching for color stereo images. *Pattern Recognit. Letters*, 28(13):1679–1687, 2007.

[12] A. Koschan, V. Rodehorst, and K. Spiller. Color stereo vision using hierarchical block matching and active color illumination. In *Proc. Int. Conf. Pattern Recognit.*, volume 1, pages 835–839, Vienna, Austria, Aug. 1996.

[13] K. Mühlmann, D. Maier, J. Hesser, and R. Männer. Calculating dense disparity maps from color stereo images, an efficient implementation. In *IEEE Workshop Stereo and Multi-Baseline Vision*, pages 30–36, Kauai, US, Jun. 2001.

[14] L. Alvarez and J. Sánchez. 3-D geometry reconstruction using a color image stereo pair and partial differential equations. Technical report, Cuadernos del Instituto Universitario de Ciencias y Tecnologas Cibernticase, Las Palmas, 2000.

[15] L. Alvarez, R. Deriche, J. Sánchez, and J. Weickert. Dense disparity map estimation respecting image discontinuities: A PDE and scale-space based approach. Technical report, INRIA, 2000.

[16] A. Koschan. Improving robot vision by color information. In *Proc. Int. Conf. Artifi. Intell. and Information Control Systems of Robots*, pages 247–258, Smolenice Castle, Slovakia, 1997.

[17] T. Belli, M. Cord, and S. Philipp-Foliguet. Colour contribution for stereo image matching. In *Proc. Int. Conf. Color in Graphics and Image Process.*, pages 317–322, Saint-Etienne, France, Oct. 2000.

[18] J. R. Jordan and A. C. Bovik. Computational stereo vision using color. *IEEE Control Systems Magazine*, 8(3):31–36, 1988.

[19] A. Koschan. Dense stereo correspondence using polychromatic block matching. In *Proc. Int. Conf. Comput. Analysis of Images and Patterns*, volume 719, pages 538–542, Budapest, Hungary, Sept. 1993.

[20] S. Chambon and A. Crouzil. Color stereo matching using correlation measures. In *Complex Systems Intelligence and Modern Technological Applications*, pages 520–525, Cherbourg, France, 2004.

[21] M. Bleyer, S. Chambon, U. Poppe, and M. Gelautz. Evaluation of different methods for using colour information in global stereo matching approaches. In *The Congress of the International Society for Photogrammetry and Remote Sensing*, Beijing, Chine, July 2008.

[22] A. Fusiello, E. Trucco, and A. Verri. A compact algorithm for rectification of stereo pairs. *Int. J. Machine Vis. and Applications, MVA*, 12(1):16–22, juillet 2000.

[23] P.L. Combettes. A block iterative surrogate constraint splitting method for quadratic signal recovery. *IEEE Trans. Signal Process.*, 51(7):1771–1782, July 2003.

[24] E. Geoffrey and P.W. Richard. Detecting binocular half-occlusions: Empirical comparaisons of five approaches. *IEEE Trans. Pattern Anal. Machine Intell.*, 42(8):1127–1133, Aug. 2002.

[25] A. L. Yuille and T. Poggio. A generalized ordering constraint for stereo correspondence. *Technical Report AIM-777*, 1984.

[26] A.N. Tikhonov and A.Y. Arsenin. Solution of ill-posed problems. *John Wiley and Sons*, 1977.

[27] L.I. Rudin, S. Osher, and E. Fatemi. Nonlinear total variation based noise removal algorithms. *Physica D*, 60:259–268, 1992.

[28] P.L. Combettes and J.C. Pesquet. Image restoration subject to a total variation constraint. *IEEE Trans. Image Process.*, 13(9):1213–1222, 2004.

[29] H.H. Nagel and W. Enkelmann. An investigation of smoothness constraints for the estimation of displacement vector fields from image sequences. *IEEE Trans. Pattern Anal. Mach. Intell.*, 8:565–593, 1986.

[30] L. Alvarez, J. Weickert, and J. Sánchez. Reliable estimation of dense optical flow fields with large displacements. *Int. J. Computer Vis.*, 39(1):41–56, 2000.